Food Hydrocolloids 145 (2023) 109064

Contents lists available at ScienceDirect

Food Hydrocolloids

journal homepage: www.elsevier.com/locate/foodhyd

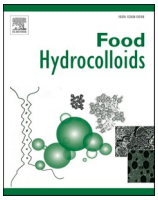

Encapsulation and stabilization of lactoferrin in polyelectrolyte ternary complexes

Tiantian Lin [a], Yufeng Zhou [a], Younas Dadmohammadi [a], Mohammad Yaghoobi [a], Gopinathan Meletharayil [b], Rohit Kapoor [b], Alireza Abbaspourrad [a,*]

[a] Department of Food Science, College of Agriculture and Life Sciences, Cornell University, Ithaca, NY, USA
[b] Dairy Management Inc., Rosemont, IL, USA

ARTICLE INFO

Keywords:
Lactoferrin
Ternary complex
Coacervate
Multiphase coacervate
Thermal stability
Antibacterial activity

ABSTRACT

Effective delivery of the bioactive protein, lactoferrin (LF), remains a challenge as it is sensitive to environmental changes and easily denatured during heating, restricting its application in functional food products. To overcome these challenges, we formulated novel polyelectrolyte ternary complexes of LF with gelatin (G) and negatively charged polysaccharides, to improve the thermal stability of LF with retained antibacterial activity. Linear, highly charged polysaccharides were able to form interpolymeric complexes with LF and G, while coacervates were formed with branched polysaccharides. A unique multiphase coacervate was observed in the gum Arabic GA-LF-G complex, where a special coacervate-in-coacervate structure was found. The ternary complexes made with GA, soy soluble polysaccharide (SSP), or high methoxyl pectin (HMP) preserved the protein structures and demonstrated enhanced thermal stability of LF. The GA-LF-G complex was especially stable with >90% retention of the native LF after treatment at 90 °C for 2 min in a water bath or at 145 °C for 30 s, while the LF control had only ~7% undenatured LF under both conditions. In comparison to untreated LF, LF in ternary complex retained significant antibacterial activity on both Gram-positive and Gram-negative bacteria, even after heat treatment. These ternary complexes of LF maintained the desired functionality of LF, thermal stability and antibacterial activity, in the final products. The ternary complex structure, particularly the multiphase coacervate, may serve as a template for the encapsulation and stabilization of other bioactives and peptides.

1. Introduction

Protein encapsulation is a growing area of interest since emerging molecular biology studies have highlighted the therapeutical functions of proteins and peptides (Ma, 2014; Scott et al., 2012). Encapsulation has led to the breakthroughs using proteins in the areas of disease prevention and treatment, drug delivery, personal care products, pharmaceuticals, and functional foods. However, effective and efficient delivery of proteins remains challenging due to their environmental sensitivity and easy denaturation (McClements, 2018). Naturally present in aqueous form, such as biological fluids, protein molecules can be stabilized through a combination of various chemical bonds and intermolecular interactions, such as hydrogen bonding, hydrophobic/hydrophilic interactions, or disulfide bonds (Blocher McTigue & Perry, 2020). These interactions, which stabilize the protein structures, can be easily affected by different pH levels and thermal conditions during the formulation and production process. Thus, encapsulation methods that take advantage of these interactions, but do not change the native protein structure and functionality, are sought.

Various strategies have been developed to protect protein and improve its stability and delivery towards heat and pH. These methods include oil-in-water and water-in-water emulsions, physical and/or chemical entrapment in nano- or microparticles/gels, liposomes, and encapsulation by segregating aqueous two-phase systems (ATPSs) and associative complex coacervates (Balcão et al., 2013; Vergara & Shene, 2019). Major concerns for these protein encapsulation methods include the use of organic solvents and low protein encapsulation efficiency, and poor loading ratios (Blocher McTigue & Perry, 2020). For example, ATPS, liposomes, and particle/gel systems are not commonly used since these systems tend to provide low loading efficiency and use organic solvents, such as ethanol, which can cause denaturation and inactivation of the protein (Kendre & Satav, 2019; Lin et al., 2021). The emulsification method is also limited as it suffers from the use of oils, synthetic emulsifiers, and complicated fabrication procedures (McClements,

* Corresponding author.
E-mail address: alireza@cornell.edu (A. Abbaspourrad).

https://doi.org/10.1016/j.foodhyd.2023.109064
Received 24 April 2023; Received in revised form 12 June 2023; Accepted 8 July 2023
Available online 11 July 2023

2018). Associative complex coacervation, however, is considered a simple, gentle process that occurs only in aqueous solutions and can achieve a high protein encapsulation yield (Blocher McTigue & Perry, 2020).

Complex coacervation is known as a liquid-liquid phase separation phenomenon driven mainly by electrostatic interactions between oppositely charged polyelectrolytes (Turgeon & Laneuville, 2009). As a result, the polymer dense liquid phase, the coacervate or pellet, will separate from the polymer-poor phase, the aqueous or supernatant phase. This phenomenon was first observed and reported in the coacervate formed by natural biopolymers gelatin (G) and gum Arabic (GA) (Bungenberg de Jong & Kruyt, 1929). Since then, many complex coacervate systems have been explored in natural biopolymers, including pectin, alginate, and chitosan. Specifically, for protein encapsulation purposes, the binary complex coacervation between protein and polysaccharide has been widely investigated (Bokkhim et al., 2016a; Bokkhim et al., 2016b; da S. Gulão et al., 2014; Niu et al., 2019). In addition to binary complex coacervation, it has been reported that charged protein encapsulation can be done by forming a ternary complex coacervate via two oppositely charged polypeptides (McTigue & L. Perry, 2019). Such ternary complex systems achieved complexation in a broader range of biopolymer compositions than the binary complex coacervate, which is known to only occur in a narrow range of mixing ratios and pH conditions (McTigue & L. Perry, 2019; Priftis et al., 2014). Furthermore, it is easy to tune the ratios of two kinds of polypeptides and the loading ratios of protein to achieve high protein encapsulation efficiency (Black et al., 2014; McTigue & L. Perry, 2019). However, the current understanding of ternary complex coacervation has been primarily limited to one protein with two oppositely charged polypeptides, and it has only rarely been observed between two oppositely charged natural biopolymers, possibly due to their relatively higher structural complexity. Furthermore, the effect of ternary complexes on the protection of protein stability has been rarely studied.

In recent years, there has been an increasing interest in broadening the application of lactoferrin (LF) in drugs, pharmaceuticals, functional foods, and health products because of its antibacterial and antiviral properties, and its ability to prevent SARS-CoV-2 viral infections (Mirabelli et al., 2021; Vogel, 2012; Wotring et al., 2022). However, LF is sensitive to thermal denaturation, especially under neutral pH conditions, which is the pH for most food products like dairy foods (Lin et al., 2022; Wang et al., 2019). LF has a positive charge (pI: 8.0–9.0) in a broad pH range below pH 7 which enables it to form electrostatic complexes with various anionic polysaccharides. The complex coacervation of LF with soy soluble polysaccharides (SSP) and GA was shown to improve the thermal stability of LF by preventing secondary structural changes (da S. Gulão et al., 2014; Lin et al., 2022).

To date, no studies have been done to investigate the formulation of ternary complexes to encapsulate and stabilize LF. Therefore, we used LF as the target protein to study the formation conditions, resulting structures, and physicochemical properties of protein-polysaccharide ternary complexes, and to probe the thermal stability of LF within those ternary complex systems. Gelatin (G) was selected as the other cationic biopolymer in the ternary complex system as it can form complex coacervates with many polysaccharides, and it is widely used as a food ingredient for human consumption (de Jong & van de Velde, 2007). Five different anionic polysaccharides (PS), including SSP, GA, high methoxyl pectin, kappa carrageenan, and iota carrageenan, were chosen as the third component of the system. SSP was chosen as a sustainable ingredient from soy byproducts and other PSs were chosen considering they are commonly used natural PSs. These PSs were investigated because of the differences in their charge density (number of charges per monosaccharide) and chain flexibility (branched *vs.* linear) as both factors are determining factors in the microstructural formation and properties of the electrostatic protein-polysaccharides complex (Chang et al., 2017; de Jong & van de Velde, 2007).

We report here the formulation of ternary complexes of positively charged LF and G with five different negatively charged polysaccharides to improve the structural stability and antibacterial activity of LF following thermal processing. We hypothesized that a ternary complex could be formed by LF, gelatin, and polysaccharides due to electrostatic interactions at optimal conditions (ratios, concentrations, and pH). The complexes formed by polysaccharides with different charge density and chain flexibility demonstrated different structures and thermal stability. Lastly, we hypothesized that the ternary complexes formed would show improved stability and retain the antibacterial activity of LF after heating process compared to LF samples. The physicochemical properties of these ternary complexes were investigated using turbidity, zeta-potential and particle size, and microscopic analysis. The structural changes and retention ratios of LF after thermal treatment were then evaluated through intrinsic fluorescence, circular dichroism (CD) spectroscopy, SDS-PAGE, and HPLC.

2. Materials and methods

2.1. Materials

Bovine Lactoferrin (LF) (Bioferrin 2000; Iron >15 mg/100g) was obtained from Glanbia Nationals, Inc. (Fitchburg, WI, USA). Soy soluble polysaccharide (SSP) was provided by Fuji Oil (Izumisano-shi, Japan). High methoxyl pectin (HMP), Kappa carrageenan (Kappa), and Iota carrageenan (Iota) were provided by Tic gum (Riverside, MD, USA). Gum Arabic (GA) was provided by Colony Gum (Monroe, NC, USA). Gelatin (Knox unflavored gelatin) was purchased from the local grocery store (Target, Ithaca, NY, USA). Fluorescein isothiocyanate isomer I (FITC) was purchased from Sigma-Aldrich (St. Louis, MO, USA). Trifluoroacetic acid, acetonitrile (HPLC grade), hydrochloric acid, sodium hydroxide, and dimethyl sulfoxide (DMSO) were purchased from Fisher Scientific (Hampton, NH, USA). The reagents for SDS-PAGE were purchased from Bio-Rad Laboratories (Hercules, CA, USA). Bicinchoninic acid (BCA) Assay Kit II was purchased from BioVision (Waltham, MA, USA). Coomassie Brilliant Bule G-250 was purchased from bioWORLD (Dublin, OH, USA). Luria broth (LB) and LB agar were purchased from Sigma-Aldrich (St. Louis, MO, USA). Other chemicals and reagents were purchased from Fisher Scientific (Hampton, NH, USA).

2.2. Preparation of ternary complex

LF, SSP, and GA solutions were prepared at 1 and 0.2 w/v % by dissolving the powders into Milli-Q water with mixing for 2 h at 25 °C. HMP, Kappa, and Iota solutions were prepared at 0.2 w/v % by dissolving the powder in warm water Milli-Q water (60 °C) with mixing for 2 h. Gelatin solutions were prepared at 1 and 0.2 w/v % by dissolving the biopolymer into Milli-Q water, heated to 60 °C, and mixing for 2 h. All solutions cooled to 4 °C and allowed to sit overnight to ensure full hydration.

The ternary complexes were prepared at a total concentration of 1 and 0.2 w/v % by proportionally adding the prepared biopolymer solutions at the same concentration (1 or 0.2 w/v %). The proportion of biopolymers was designed according to the ternary plot with a ratio interval of 10% (Priftis et al., 2014). All the biopolymer solutions were adjusted to the starting target pH levels: pH 4 and pH 7. These pH levels were selected to represent the pH when LF has a high positive charge (pH 4) and a low positive charge (pH 7). Different polysaccharide solutions were mixed with LF solutions first for 30 min at 25 °C to form the intermediate complex. Then the mixtures were heated to 45 °C and mixed with preheated gelatin solutions at 45 °C for another 30 min.

The ternary complexes were obtained by centrifuging the ternary mixtures at 10,000*g* for 25 min at 4 °C. The complex pellets were collected and frozen at −20 °C for at least 12 h and then freeze-dried (Labcono, Kansas, MO, USA). The supernatant was retained for complexation efficiency measurements.

2.3. Characterization of complex

2.3.1. Turbidity measurements

The transmittance of the ternary mixtures was measured at 600 nm using a UV–Vis spectrophotometer (UV-2600, SHIMADZU Co., Japan) according to (Zheng et al., 2020). Samples were analyzed in a quartz cuvette (1-cm path-length). The turbidity was calculated based on the equation below (**Eq. (1)**):

$$Turbidity = -\ln\frac{I}{I_0} \quad \text{(Eq.1)}$$

where I is the transmittance intensity of samples and I_0 is the transmittance intensity of blank (i.e., Milli-Q water).

2.3.2. Particle size and zeta-potential measurements

The average particle diameter and zeta-potential of the ternary mixtures were measured by the Zetasizer Nano-ZS (Malvern, Germany) using the same method as described by (Lin et al., 2022). Samples were analyzed in triplicate.

2.3.3. Morphology characterization

2.3.3.1. Confocal microscopy analysis. LF was labeled with FITC (Fluorescein isothiocyanate) for imaging purposes using the following procedure. LF was dissolved in 10 mM carbonate buffer (pH 10.0) at 5 w/v %. FITC was dissolved in DMSO at 10 w/v %. The LF solution was mixed with FITC at a volume ratio of 20:1 for 3–4 h at room temperature in the dark. The mixture was washed through a gel filtration column (filled with Sephadex G-25) to remove the excessive FITC. The green-yellow solution was collected from the column and confirmed with the labeled protein by UV–vis spectroscopy. The obtained FTIC-labeled LF solution was freeze-dried for later use in the ternary complexes and confocal microscopy analysis.

The confocal microscopy images of the ternary complex made with FTIC-labeled LF were obtained using the Zeiss LSM 710 confocal laser scanning microscope connected to Inverted Axio Observer.Z1 microscope, using a 40 × water immersion objective (NA 1.2). A small aliquot of the complex solutions was transferred to a glass microscope slip and covered with a glass coverslip. Green (confocal) images allowed us to visualize LF in the complexes by using the excitation argon laser (488 nm) and detection light between 500 and 559 nm. Regular optical images were taken by turning off the laser and turning on the regular white polarized light. The images were analyzed by the instrument software (EZ CS1 version 3.8, Niko, Melville, NY).

2.3.3.2. Scanning electron microscopy analysis. The microstructure of the LF ternary complex was visualized using a Field-emission scanning electron microscope (SEM) (Zeiss Gemini 500, Jena, Germany) by the method as described by (Lin et al., 2022). Before taking the microscopy images, fresh ternary mixture samples (~10 μL) were vacuum-dried overnight and then coated with Au/Pd in a sputter coater (Denton Desk V, NJ, USA).

2.3.4. Measurement of complexation efficiency, yield, and loading ratio of LF

The supernatant obtained after centrifuging the ternary mixtures was appropriately diluted and used to quantify the free LF according to the Bradford method (Bradford, 1976). The complexation efficiency was calculated according to the following equation (**Eq. (2)**):

$$Complexation\ efficiency\ (CE)\% = 100 \times \frac{Total\ LF - Free\ LF}{Total\ LF} \quad \text{(Eq. 2)}$$

Total LF was the theoretical concentration (w/v %) of LF employed in the ternary mixture; Free LF was the measured concentration (w/v %) of LF in the supernatant.

The freeze-dried complex samples were weighed for yield measurement, which was calculated according to the following equation (**Eq. (3)**):

$$Yield\ (\%) = 100 \times \frac{Mass\ of\ freeze-dried\ complex}{Mass\ of\ total\ soild\ in\ biopolymer\ solutions} \quad \text{(Eq. 3)}$$

The loading ratio (mass ratio) of LF in the freeze-dried complex samples was quantified in the redispersed complex samples in PBS buffer pH 7 at a concentration of 0.2 w/v % using the BCA assay. The loading ratio of LF in the freeze-dried complex was calculated according to the following equation (**Eq. (4)**):

$$Loading\ ratio\ of\ LF\ (\%) = 100 \times \frac{Concentration\ of\ LF\ in\ complex\ solution\ (w/v\%)}{Complex\ concentration\ (0.2 w/v\%)} \quad \text{(Eq.4)}$$

2.3.5. Thermal stability test of LF in the ternary complex

The thermal stability of pure LF and LF in ternary complex under neutral pH were measured and compared. Pure LF and freeze-dried ternary complex were first dispersed in 10 mM PBS buffer at pH 7 (0.2 w/v %) and then transferred into glass tubes (2 mL). Samples were heated in the water baths at 75 °C or 90 °C for 2 min and then immersed in an ice-water bath for several minutes until the samples were cooled to ambient temperature (T ~ 25 °C) before further analysis. Samples were also processed at 145 °C using an oil bath and were processed at this temperature for 2 s, 10 s, 30 s, and 60 s. The optical images, turbidity, zeta-potential, and particle size of the sample solutions before and after heating were measured. Intrinsic fluorescence and circular dichroism spectroscopy were analyzed to understand the structural changes of the protein during heating. Electrophoresis analysis and HPLC analysis were used to quantify the LF retention rate after thermal treatment.

2.3.6. Circular dichroism (CD) spectroscopy

The secondary structures of LF in pure LF and ternary complex solutions before and after heating were measured using CD spectroscopy by an AVIV-202-01 spectropolarimeter (Lakewood, NJ, USA). Samples were measured in the far-UV region (190–260 nm) at 25 °C in a 1-mm path length quartz cell. Samples were diluted to ~0.02 w/v % of protein before measurement. Pure gelatin showed no secondary structures according to its limited CD spectra signal; therefore, the CD spectra of the ternary complex was mainly referred to as the secondary structures of LF.

2.3.7. Intrinsic fluorescence spectroscopy

The intrinsic fluorescence of pure LF and LF in the ternary complex solutions, before and after heating, was measured using a Shimadzu RF-6000 spectrophotometer (Shimadzu, Japan). Samples were measured in a 1-cm quartz cuvette at an excitation wavelength of 295 nm and emission wavelength range of 310–400 nm with a 10 nm scanning interval, to obtain the intrinsic fluorescence of the protein's aromatic tryptophan residues.

2.3.8. Electrophoresis analysis

Unheated and heated LF and the ternary complex samples were analyzed using sodium dodecyl sulfate (SDS)-PAGE in a vertical mini gel electrophoresis system (Mini-PRO-TEAN Tetra cell, Bio-Rad, USA) using the protocol described by (Lin et al., 2022).

2.3.9. Quantification of LF by HPLC

An HPLC method was developed to quantify the undenatured LF in complex solutions after thermal treatment. The liquid above the protein aggregates was sampled and filtered (0.22 μm) for HPLC analysis. LF separation was performed using the reversed-phase BioZen Intact XB-C8 HPLC column (150 × 4.6 mm, 3.6 μm; Phenomenex, Torrance CA, USA) at 40 °C in the Agilent 1100/1200 series HPLC system (Agilent Technologies, CA, USA). Detection was carried out at 214 nm by a diode

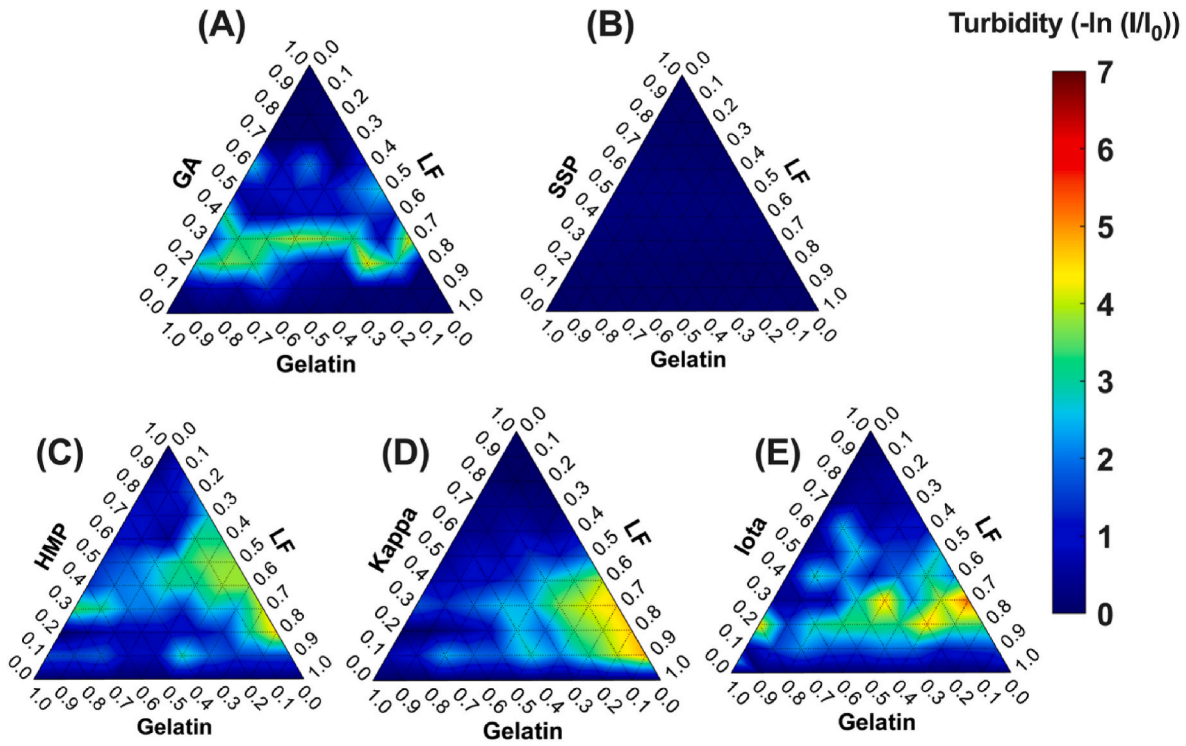

Fig. 1. Plots of turbidity for ternary mixtures including lactoferrin (LF), gelatin (G), and a polysaccharide (PS) selected from gum Arabic (GA), soy soluble polysaccharides (SSP), high methoxyl pectin (HMP), kappa carrageenan (Kappa), and iota carrageenan (Iota) (A–E) as a function of compositions in mass ratios (0–1) at a total concentration of 0.2 w/v% at pH 4.

array detector. A gradient elution was performed using 0.1 v/v % trifluoroacetic acid (TFA) in water (mobile phase A) and 0.1 v/v % TFA in Acetonitrile (mobile phase B) at a flow rate of 1.0 mL/min using the following gradient elution: 0–20 min, 5–50% B; 20–21 min, 50% B; 21–25 min, 50-5% B. The injection volume was 10 μL. The concentration of remaining native LF in sample solutions can be measured and quantified according to a standard curve of native LF with a concentration of 0–0.2 w/v % (R^2 >99%). The LF retention rate, which indicates how much LF remains native after thermal treatment in the complex solution, was calculated using the following equation:

$$LF\ retention\ (\%) = 100 \times \frac{Concentration\ of LF\ after\ heating}{Concentraiton\ of\ LF\ before\ heating} \quad \text{(Eq. 5)}$$

2.3.10. Antimicrobial activity analysis

A strain of *Staphylococcus aureus* (*S. aureus*) and a strain of *Escherichia coli* (*E. coli*) were used in this study as target gram-positive bacteria and gram-negative bacteria. *S. aureus* was isolated by the Animal Health Diagnostic Center of Cornell University (AHDC) from bovine feces. E. coil (k12 Mg1655) was obtained from American Type Culture Collection (ACTT) (Freddolino et al., 2012). Frozen bacteria were first activated in Luria Broth (LB) agar medium. Then a loop of a pure colony was transferred and incubated into fresh LB medium for 24 h at 37 °C for further antibacterial activity measurement.

The antibacterial activity measurement was performed on a 96-well microtiter plate using the UV absorbance method. First, the bacteria, *S. aureus* or *E. coli*, were diluted in LB broth 1000 times to make sure the absorbance of 100 μL bacteria broth was less than 0.04 at 625 nm. An increase in absorbance at 625 nm (OD625) was used to indicate the growth of bacteria. For the MIC (minimal inhibitory concentration) study (Matijašić et al., 2020), LF at different diluted concentrations (0.1–1 w/v %) was used. A volume of 100 μL diluted *S. aureus* broth and 100 μL LF solution was added to each well. Then, 100 μL bacteria broth with 100 μL PBS buffer was applied as the control. The minimal concentration of LF to inhibit 50% of bacterial growth (50% of OD625 value in control) was referred to as MIC of LF on bacteria and was used as the LF concentration for further antibacterial studies of the LF ternary complex study. Similarly, 100 μL of diluted bacterial broth and 100 μL of unheated and heated LF complex solutions at the selected concentration (0.2 w/v %) were added to each well. The microtiter plate was incubated at 37 °C, and the OD625 was measured to monitor the growth of bacteria at 0, 24, and 48 h of incubation, with shaking 10 s before reading.

2.4. Data analysis

Results were displayed as means ± standard deviations. The difference between mean values was compared using the Tukey HSD test (p-value <0.05) using JMP Pro16 (SAS Institute, USA). Figures were plotted using GraphPad Prism9 (GraphPad Software Inc., USA), except for the ternary plots, which were plotted by MATLAB (R2020a, MathWorks, Natick, MA, USA).

3. Results and discussion

3.1. Effect of the polysaccharide mixing ratios and concentration on complex formation

The effect of different biopolymer mixing ratios on the formation of the ternary complexes made from a polysaccharide with LF and gelatin at pH 4 and pH 7 was investigated through turbidity, which is commonly used as a quick and simple indicator for complex formation (da S. Gulão et al., 2014). Charge density, structural characteristics, and approximate molecular weight of five polysaccharides were tabulated for reference (Table S1). In general, soy soluble polysaccharides (SSP) and gum Arabic (GA) are branched polysaccharides with a charge density lower than 0.3, while high methoxyl pectin (HMP), kappa carrageenan (Kappa), and iota carrageenan (Iota) are linear polysaccharides, with a charge density of 0.3–0.6, 0.5, and 1, respectively (de Jong & van de Velde, 2007). The total biopolymer concentration for each ternary system was the same (0.2 w/v %).

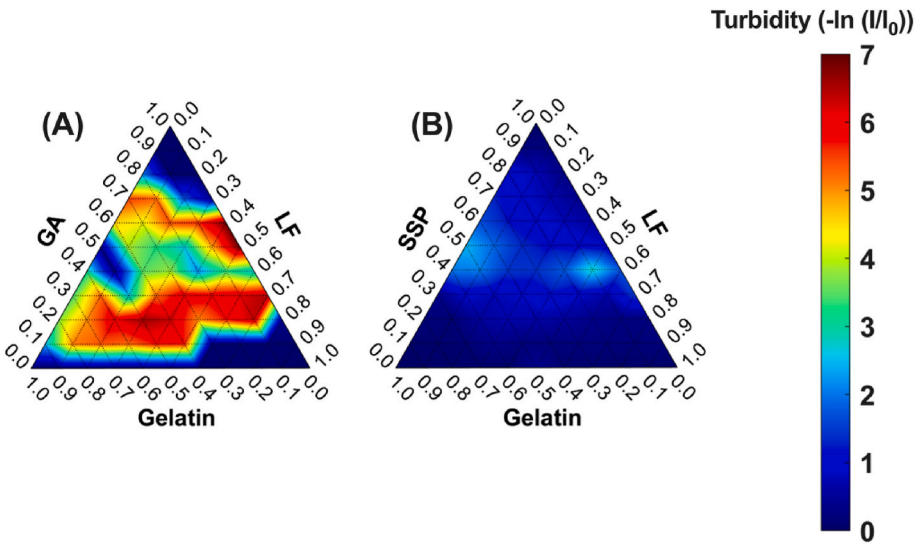

Fig. 2. Plots of turbidity for ternary GA-LF-G (A) and SSP-LF-G (B) mixtures as a function of composition in mass ratios (0–1) at a total concentration of 1 w/v % at pH 4.

A ternary plot was used to design the mixing ratio of the three biopolymers (Fig. 1); the scale for the three axes indicates the mass ratio of the biopolymers being added to the ternary mixture. A darker green to red color of the ternary mixtures at certain biopolymer ratios represented higher turbidity (3–7), which further indicates a stronger interaction and complexation formation among those biopolymers.

The different ternary systems showed different complex formation ranges; complex formation was indicated when the turbidity was found to be greater than 2 (Fig. 1). For the GA-LF-G system, a complex was formed when the mixtures consisted of 60–80% LF and 20–40% GA (Fig. 1A), while the concentration of gelatin seemed to have little effect. In general, SSP-LF-G mixtures showed a very limited complex formation in all studied conditions with relatively low turbidity, less than 3, across the range of mass ratios (Fig. 1B). For the HMP-LF-G system, a complex was formed when the mixture consisted of 30–90% of LF, 30–90% of HMP and 40–50% of gelatin (Fig. 1C). For both Kappa-LF-G and Iota-LF-G mixtures, the complex formation range was shifted to 50–90% of LF, 50–90% of Kappa or Iota, and less than 50% of gelatin (Fig. 1D and E). A higher gelatin concentration (>50%) seemed to disfavor the complex formation when linear polysaccharides were involved, showing a lower turbidity. The higher charge densities and greater number of negative charges carried by HMP, Kappa, and Iota contribute to the increased ability of these polysaccharides to form complexes with LF at high mass ratios of LF in comparison to SSP and GA (Tables S1 and S2).

Furthermore, the maximum turbidity ($Turbidity_{max}$) was different among these systems. SSP-LF-G system showed the lowest $Turbidity_{max}$. Kappa and Iota demonstrated a higher $Turbidity_{max}$ in their complex compared to other systems. The maximum turbidity represented the

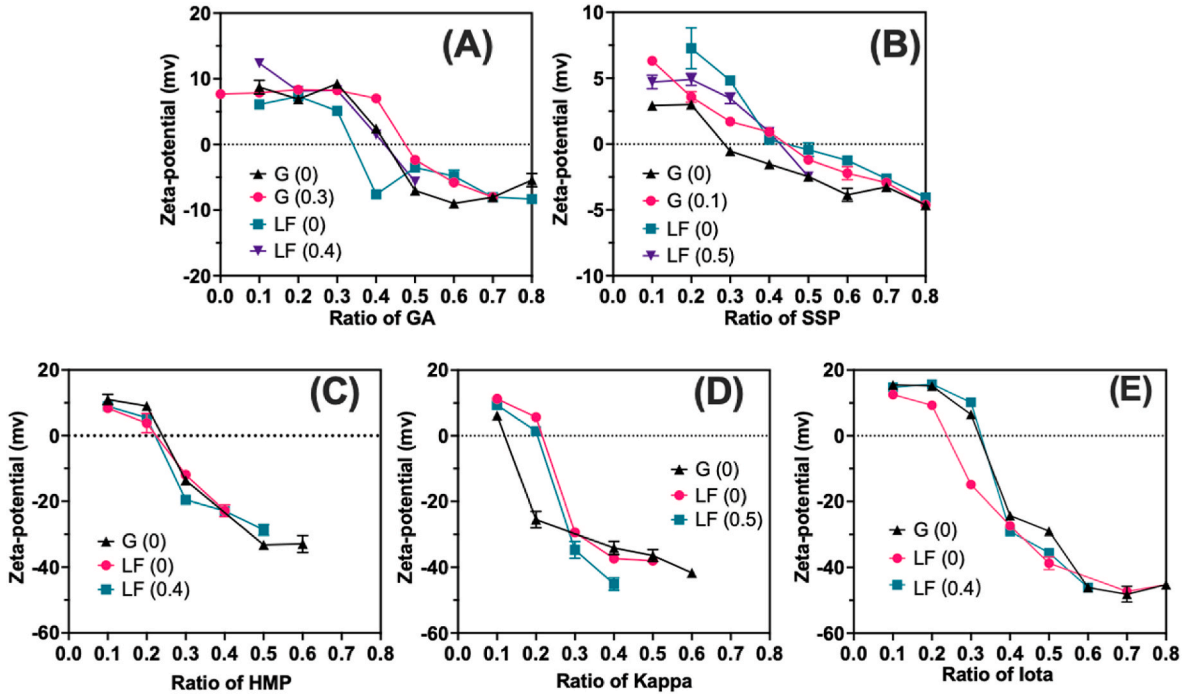

Fig. 3. The zeta-potential of PS (GA/SSP/HMP/Kappa/Iota, A-E)-LF-G mixtures at a total concentration of 1 or 0.2 w/v % at pH 4 as a function of mass ratios of PS with a fixed mass ratio of LF or gelatin (numbers in the parentheses).

maximum extent of complexation and the strength of electrostatic interactions in the system, which is related to the relative amounts of oppositely charged groups in the individual solutions. Furthermore, the complexes with three linear polysaccharides (HMP, Kappa, and Iota) were formed over a wider range of compositional ratios than the complex using branched polysaccharides (GA).

Considering the relatively low turbidity in SSP and GA systems at the total concentration of 0.2 w/v %, an increased concentration of biopolymers (1 w/v %) in these two ternary systems was further studied (Fig. 2). Increasing the concentration, which enhances the electrostatic interactions, caused the $Turbidity_{max}$ in both complex systems to increase, especially in the GA-LF-G complex (Fig. 2A). While it is expected that a higher concentration would promote a higher extent of complexation because of the increased density of opposite charges and the decreased molecular distances in solution, however, this promotion was much more significant in the GA-LF-G system and less apparent in the SSP-LF-G system. The zeta-potential, representing the charge density, of GA and SSP was very similar in 0.2 w/v % or 1 w/v % concentrations (Table S2), therefore the differences in chain flexibility, between GA and SSP, could be responsible for their observed differences in complex formation with LF and gelatin (de Jong & van de Velde, 2007).

At pH 7 regardless of biopolymer ratio or composition, the turbidity remained low (<2) which indicated that very limited complex formation was observed (data not shown). We attributed this to the low charge on LF and gelatin at pH 7 (Table S2), which limited the electrostatic interactions between LF and gelatin with the polysaccharides.

Overall, the final total concentration of the ternary complex was chosen as 1 w/v % in the ternary complex formed with GA or SSP and 0.2 w/v % in the ternary system formed with HMP, Kappa, or Iota. The pH level was fixed at pH 4 where all the biopolymers had comparatively high charges. Using the triangle turbidity plots (Figs. 1 and 2), we then selected the biopolymers ratio that provided the highest turbidity and a moderate mass ratio of the target protein, LF, as the optimal conditions for complex formation. Specifically, the optimal biopolymer mass ratios were selected as follows: GA:LF:G (2:6:2); SSP:LF:G (4:5:1); HMP:LF:G (4:5:1), Kappa:LF:G (3:6:1), Iota:LF:G (2:6:2).

3.2. Zeta-potential and particle size of the ternary complex

Ternary mixtures with fixed gelatin and LF ratios were chosen to study the effect of the addition of polysaccharides (PS) or LF on the zeta-potentials of the ternary mixtures. With the addition of negatively charged PS, the zeta-potential of the ternary mixtures gradually decreased from positive charges to zero and then further decreased into negative charges (Fig. 3). As would be expected, the ratios, when the overall zeta-potentials were close to zero, showed the highest turbidity (Figs. 1 and 2); when the overall zeta-potential reached zero, the biopolymers had a similar number of opposite charges on the surface and formed the ternary complex due to electrostatic attractions. Minimization of the repulsive interactions among the biopolymers decreased as the system had the fewer similar charges which further facilitated the formation of the larger complexes.

To explore the impact of pH and biopolymer mass ratios on the particle size of ternary complexes, we chose one branched polysaccharide, GA, and one linear polysaccharide, Iota (Table S3). The mixture of GA-LF-G at the optimal mass ratio of 2:6:2 at pH 4 showed a large mean particle size due to complex formation, while at pH 7, the same ratio showed a smaller mean size indicating limited complex formation. Similarly, the samples of Iota-LF-G at an optimal mass ratio of 2:6:2 showed an even larger mean size compared to the GA-LF-G systems because of the higher charge density of Iota, although the total concentration of the Iota system (0.2 w/v %) was lower than the GA system (1 w/v %).

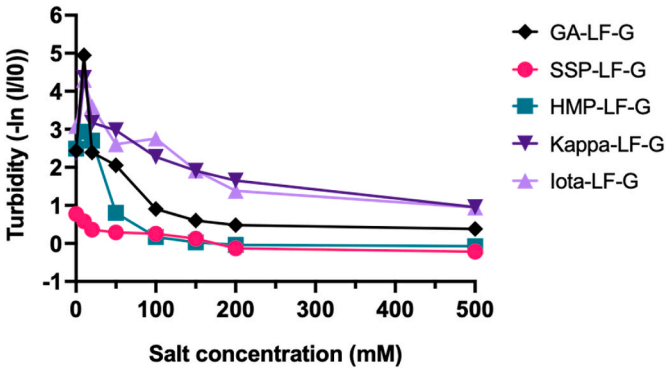

Fig. 4. The turbidity of PS (GA/SSP/HMP/Kappa/Iota)-LF-G mixtures at pH 4 as a function of salt concentration in the range of 0–500 mM.

3.3. Effect of salt concentration on the complex formation of the ternary complex

Turbidity was used to assess the effect of ionic strength (up to 500 mM) on complex formation (Fig. S1). At low salt concentrations (<50 mM), there was an increase of turbidity in all ternary mixtures (Fig. 4), except for the SSP-LF-G system that showed a low turbidity and a limited complex formation, which was consistent with the results in the ternary plot study. When the salt concentration was further increased, we observed a decrease of turbidity in all samples (Fig. 4). This observed trend in turbidity as a function of changes in salt concentration in the ternary complex is similar to those reported in binary complex systems (Anema & de Kruif, 2014; Lin et al., 2022). At lower salt concentrations, the release of the ions from between the polymers is favored and thus complex formation is also favored. However, at higher salt concentrations, the entropy gained by releasing the small ions between the biopolymers becomes unfavorable due to the charge screening effect, which results in a decreased electrostatic attraction and a lower complex formation (Blocher McTigue & Perry, 2020; da S. Gulão et al., 2014).

When the salt concentration was increased to 500 mM, the turbidity of all samples decreased to a steady level although the levels varied among different PS-LF-G mixtures (Fig. 4). The turbidity of SSP-LF-G and HMP-LF-G mixtures decreased to almost zero, which means the complexes no longer existed. GA-LF-G showed a slightly higher turbidity than SSP/HMP-LF-G, indicating the formed complex by GA-LF-G had a higher resistance to salt. The Kappa-LF-G and Iota-LF-G complexes showed the highest resistance to salt; their turbidity was the highest and it remained above 1 even when the salt concentration approached 500 mM. The wide variance in salt resistance among these ternary complexes is indicative of the strength of electrostatic interactions between the components in the system. A higher salt resistance in Kappa-LF-G and Iota-LF-G reflected stronger electrostatic interactions because of the higher charge density and the linear structures of Kappa and Iota, compared to other polysaccharides.

3.4. Complex yield, complexation efficiency, and LF loading ratio

After obtaining the optimal conditions for forming a ternary complex, the ternary mixture solutions were centrifuged and the supernatant, with un-complexed biopolymers, was removed. The resulting pellet, with complexed biopolymers, was then freeze-dried. The average yield, complexation efficiency, and final mass loading ratio of LF in the freeze-dried complex were measured (Table S4). The ternary mixtures formed with the linear, highly charged PS Kappa and Iota carrageenan showed the highest yield of complex (70–80%) with the highest complexation efficiency (96%). Conversely, the mixtures formed with the linear, less charged PS HMP provided a moderate yield of complex (~40%) and a moderate complexation efficiency (52%). The ternary mixtures formed with the branched, even less charged PS, GA and SSP,

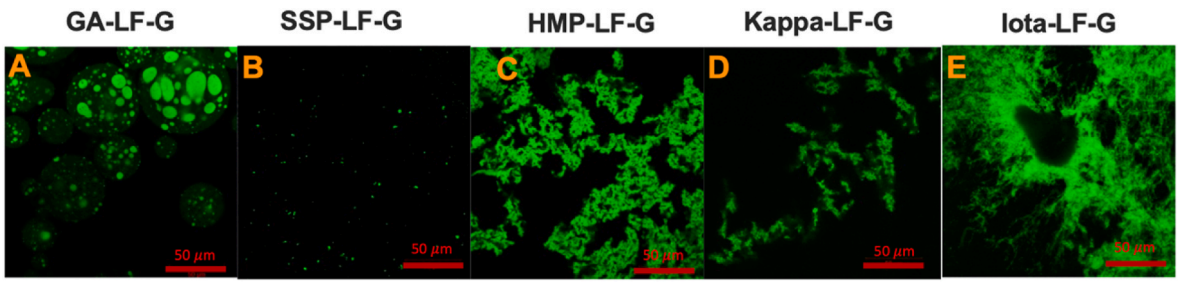

Fig. 5. The confocal microscopy images. GA-LF-G multiphase coacervates (A), SSP-LF-G coacervates (B), and HMP-LF-G, Kappa-LF-G, Iota-LF-G interpolymeric complexes (C, D and E).

showed a lower yield (40% and 17%) and a moderate to low complexation efficiency (50% and 20%). A high complexation efficiency (96%) in Kappa-LF-G and Iota-LF-G mixtures indicated that almost all LF present in the mixtures was incorporated into the complex, while GA/HMP-LF-G mixtures only incorporated ~50% of the available LF. Generally, the results showed that the complex formed with the linear and more highly charged PS, Kappa, and Iota, showed a higher yield and complexation efficiency than those formed with the more neutral PS, HMP and GA. This result is consistent with the turbidity results that highly charged polysaccharides, Kappa, and Iota carrageenan, demonstrated a higher turbidity and complex formation with LF and gelatin, indicating stronger interactions in these ternary complexes. Similarly, Jones et al studied the complexes formed by β-lactoglobulin and pectin with different charges (Jones et al., 2010). They found that at the same conditions (ratio, pH and concentration), a higher turbidity and more complex sediments were formed in mixtures made of β-lactoglobulin and low methoxyl pectin (with a higher charge), compared to the one formed by β-lactoglobulin and high methoxyl pectin (with a lower charge).

To quantify the final loading ratio (mass ratio) of LF in the complexes we used three different methods: Bradford assay, BCA (bicinchoninic acid) assay, and HPLC analysis. Our preliminary investigations indicated that the Bradford agent interacts with the sulfate groups in Kappa and Iota carrageenan, lowering the UV absorbance readings and thus underestimating the LF content. The HPLC analysis was also less useful for determining LF content in the Kappa and Iota carrageenan ternary complexes (data not shown). Strong electrostatic interactions originating from the sulfate groups in Kappa and Iota carrageenan are reported to hinder the in vitro proteolysis of lactoferrin in the gastrointestinal tract (David et al., 2020). Thus, the BCA method was chosen to quantify the mass ratio of LF in the ternary complexes. The LF loading ratio in the GA complex was ~52%, the loading in HMP complex was ~40–42%, while in the Kappa and Iota carrageenan complex was around 54–68% (Table S4). The highest LF ratio in the Kappa and Iota complexes was expected since they had a higher complexation efficiency compared to other PS-formed ternary complexes.

3.5. Morphology of ternary complex

Although many protein-polysaccharide complexes have been formed because of electrostatic interactions, their structures and properties vary according to the type of complex they form (de Jong & van de Velde, 2007). Depending on the interaction strength of biopolymers, the charge density, the molecular chain length, and the type of structures (linear, branched), three types of the protein-polysaccharide complex can form: 1) Complex coacervates (liquid phase); 2) interpolymeric complexes (co-precipitates); and 3) electrostatic gels (Rioux et al., 2007; Turgeon & Laneuville, 2009; Van Calsteren et al., 2002). Generally, coacervates are formed when the PS or protein possesses a low charge density or very flexible backbone, such as gelatin, acacia gum, and gum Arabic. Two liquid phases are formed, but due to the retention of the original solvent, they remain in solution. Conversely, interpolymeric complexes form when the PS or the protein in the system is highly charged or has a very stiff linear structure, such as carrageenan, and the complex separates from the liquid phase and precipitates, which is why these complexes are often called co-precipitates (Turgeon & Laneuville, 2009). For example, coacervate complexes are formed by β-lactoglobulin and neutral PS, while interpolymeric complexes were formed when the PS was anionic (Rioux et al., 2007; Schmitt et al., 2001; Van Calsteren et al., 2002). Even though it is not fully understood why some protein and PS systems form coacervates versus interpolymeric complexes, the formation of the interpolymeric complex may be related to a larger binding affinity between biopolymers than the individual biopolymers to the solution counterions (Turgeon & Laneuville, 2009). We have observed a similar phenomenon in the current study.

Our ternary complexes were visualized using confocal microscopy (Fig. 5) and SEM (Fig. S1). The GA-LF-G ternary complex showed multiphase coacervate droplets (Lu & Spruijt, 2020), with GA-LF coacervate droplets inside a larger GA-G coacervate droplet (Fig. 5A), which has not been reported in protein-polysaccharides complex coacervates. LF, as labeled by FITC (green), was predominately located inside the multiphase coacervate in the form of a GA-LF coacervate. The SEM of the GA-LF-G complexes after overnight vacuum drying (Fig. S1) showed the GA-LF-G complex as a compressed flat particle due to the water evaporation, indicating the liquid-like properties of coacervates. In confocal images, a scattering of SSP-LF-G nano-sized coacervate particles can be seen, indicative of the low yield (8%) of SSP-LF-G complexes formed, while the HMP-LF-G, Kappa-LF-G, and Iota-LF-G complex all showed the characteristic morphology associated with dense interpolymeric network structures (Fig. 5). The SEM images confirmed the interpolymeric complex structure of the ternary complex using these three linear polysaccharides, HMP, Kappa and Iota (Fig. S1).

Although multiphase coacervate droplets have been reported in biological systems (Fisher & Elbaum-Garfinkle, 2020; Lu & Spruijt, 2020; Mountain & Keating, 2020), to the best of our knowledge, this is the first time that this kind of phenomenon was observed in food grade biopolymers (GA-LF-G complex), specifically protein-polysaccharides systems. The major driving forces to form a coacervate complex in multiphase droplets are reported to be the different critical salt concentrations and densities between the outer coacervate and the inner coacervate (Lu & Spruijt, 2020). Such novel coacervate-in-coacervate complex structures may have potential to overcome some of the shortcomings of commonly used delivery systems that are good at delivering small bioactive molecules but not as good for charged macromolecules.

3.6. Thermal stability of LF in the ternary complex

3.6.1. Optical images, turbidity, and particle size of LF ternary complex after thermal treatment

After optimizing the formulation conditions of ternary complexes and characterizing their morphology, the second goal of this study is to evaluate the thermal stability of LF in these complex formulations. LF is known to be easily denatured under thermal processing conditions, especially at a neutral pH (Goulding et al., 2021). Thus, to exam the

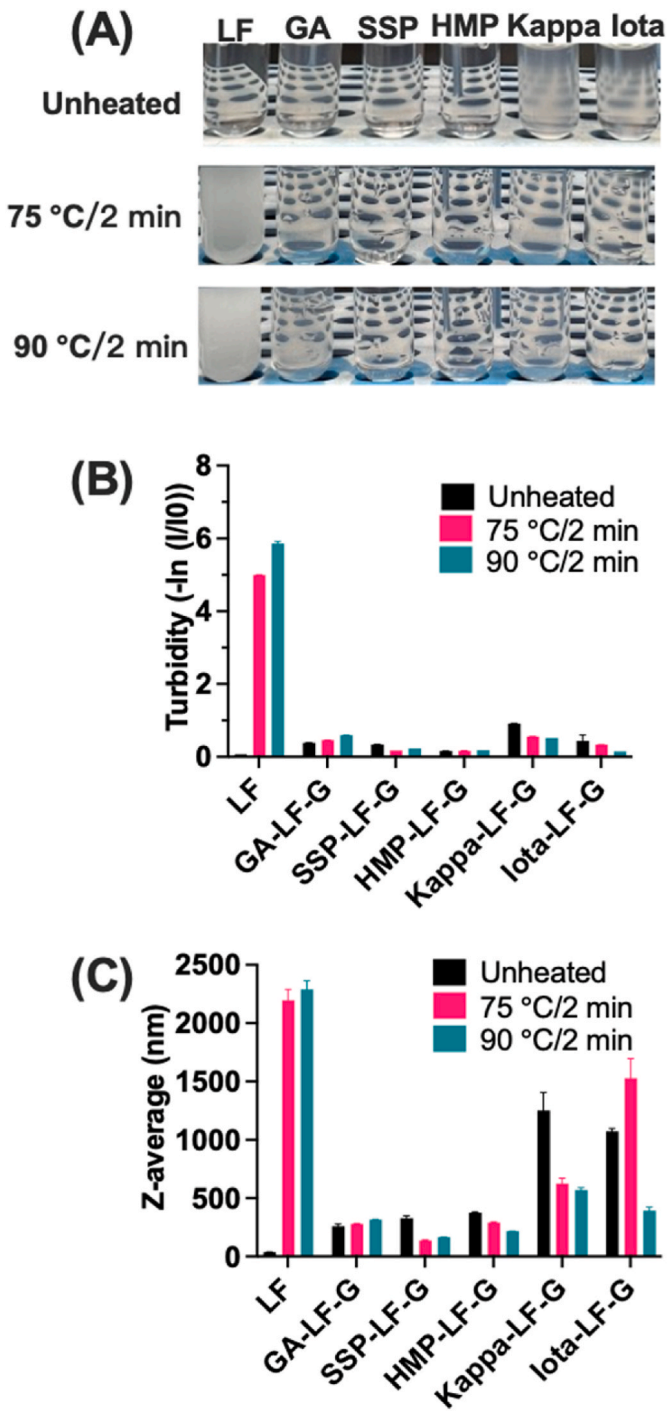

Fig. 6. The photographs (A), turbidity (B), and mean particle size (C) of unheated and heated (75 °C/2 min or 90 °C/2 min) LF and re-dispersed ternary complexes in PBS (10 mM, pH 7).

thermal stability of LF in complex samples, the freeze-dried complexes were re-dispersed at 0.2 w/v % in 10 mM PBS buffer (pH 7) and the solutions were then thermally treated in a water bath at two different temperatures (75 °C/2 min and 90 °C/2 min) that approximate the pasteurization conditions of neutral milk-based beverages (IDFA, 2022). Pure LF was easily denatured in PBS buffer at pH 7 at 75 °C, while at 90 °C the solution was even more turbid with a higher degree of precipitate formed (Fig. 6A). Compared to pure LF, the LF complexes under the same treatment conditions demonstrated much clearer solutions. This can be more directly observed in the measured turbidity that shows pure LF had a large increase of turbidity from less than 0.5 to greater than 4 after being heated, while the turbidity change of LF in the complexes was limited, less than 1 for all (Fig. 6B). The aggregation of LF proteins, when LF was heated by itself, caused a significant increase in particle size increasing from less than 100 nm to greater than 2000 nm, while in the ternary complexes formed by GA, SSP, or HMP the change in particle size was small less than 500 nm (Fig. 6C). Conversely, the complex formed by Kappa and Iota had a larger particle size than other complexes when re-dissolved in buffer solution and showed a decrease in particle size after thermal treatment (Fig. 6C). As pointed out previously the complex formed by kappa and iota carrageenan showed strong interactions between LF and G, which enabled them to form larger particles and thus showed a lower solubility in solutions. We postulate that the heating process could induce the breakdown of the large ternary complexes into smaller complex particles thus improving their solubility and reducing their overall particle size. They were still considered complexes, however, as their particle sizes were still larger than the particle size of native LF, which was measured to be ~60 nm. All of the re-dispersed complexes showed a reduced particle size ranging from 200 to 1000 nm before heating. This indicated that the complexes, which were formed at pH 4 and deposited/aggregated upon centrifugation and freeze-drying process, were broken into smaller complex clusters with improved dispersity at pH7 because of the reduced complexation strength.

3.6.2. Structural changes of LF in the ternary complex after thermal treatment

The CD spectroscopy of LF ternary before and after thermal treatment was measured to assess secondary structure changes of LF during thermal treatment. Pure native LF had a positive peak at 196 nm and a negative peak at 210 nm, indicating the α/β structure of the LF protein (Figs. S2–A). LF is reported to consist of 16–20% of α-helix, 33–42% of β-strands, 10–12% of β-turns, and 30–34% of unordered structures (Lin et al., 2022; Wang et al., 2017). After thermal treatment, pure LF showed a significant decrease in peak intensity at 210 nm, indicating the loss of α-helix, a similar change was reported by previous studies (Goulding et al., 2021; Lin et al., 2022). The higher the heating temperature, the larger the decrease of the 210 nm peak intensity. After being heated at 90 °C/2 min, the CD spectra signal, and the peak intensity of LF were very low, indicating a high degree of degradation and significant loss of the LF α-helix. However, the CD spectra for all the complex solutions was largely unaffected even after being heated up to 90 °C, indicating that the secondary structure of LF was well preserved in the complex solutions during the heating process (Figs. S2–F). Particularly, the CD spectrum of GA-LF-G complex solutions barely changed after thermal treatment, showing a high degree of preservation of LF native structures (Figs. S2–B). Our previous work also found improved thermal stability of LF secondary structures by complexation with negatively charged soluble soy polysaccharides (Lin et al., 2022); however, such limited change of secondary structures of LF demonstrated in current GA-LF-G samples has not been reported previously.

To further understand the conformational changes of LF in the system after the heating process, the intrinsic fluorescence of unheated and heated (75 °C/2 min) samples was investigated (Fig. 7A and B). The fluorescence emission maximum peak of pure LF after heating showed a red shift from 333 to 339 nm in the fluorescence spectrum (Fig. 7A). This red shift is typical and accounted for by the increased exposure of tryptophan residues from the unfolded protein to the solvent indicating that LF is unfolding during the heating process (Sreedhara et al., 2010). Further, the peak intensity of LF was increased by 29% (Fig. 7C) after being heated at 75 °C for 2 min, indicating the reduced quenching of tryptophan by adjacent amino acids when LF unfolds (Royer, 2006). A redshift and a peak intensity increase in the fluorescence spectrum of LF upon heating has also been reported by Osel (Osel et al., 2021). After thermal treatment, the emission peak of the complex samples showed a smaller redshift indicating less protein unfolding (Fig. 7C). The increase

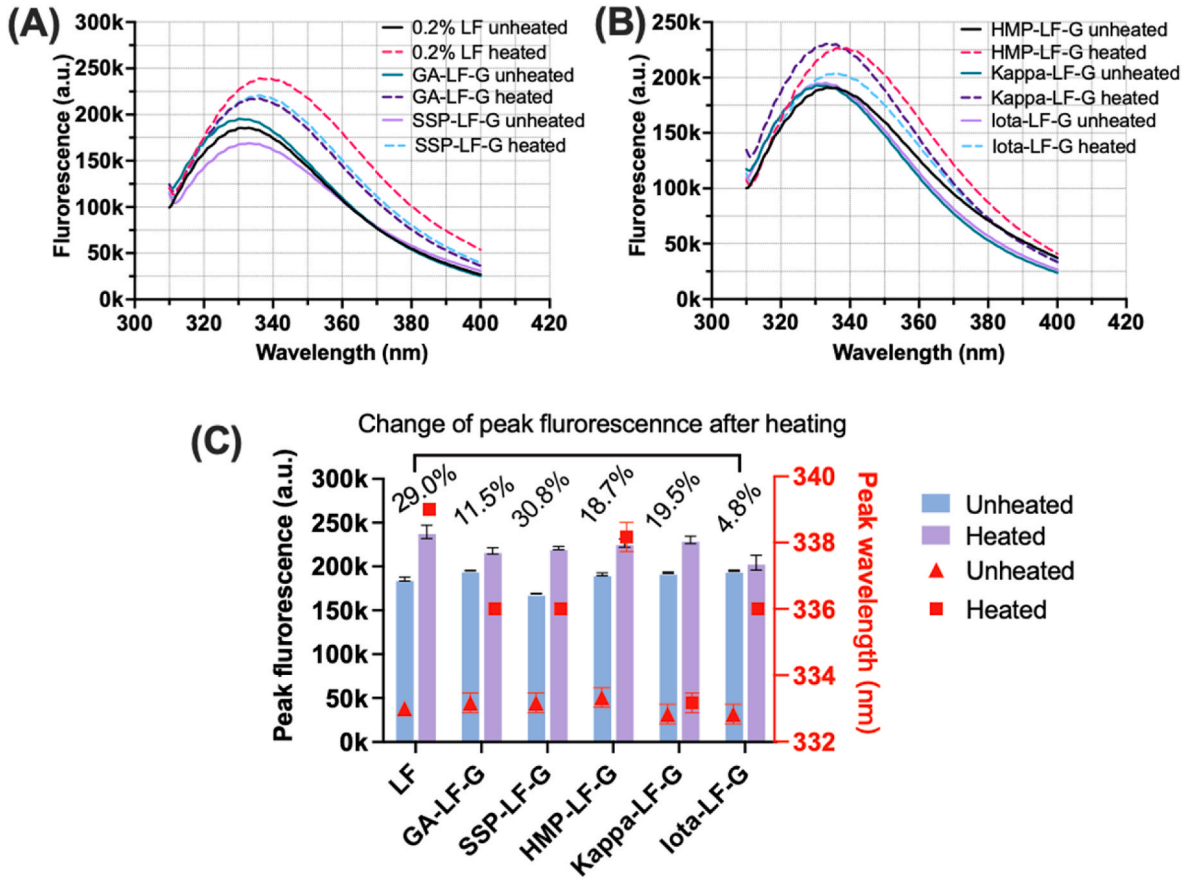

Fig. 7. The intrinsic fluorescence (A and B) and peak fluorescence (C) for unheated and heated (75 °C/2 min) LF and re-dispersed ternary complexes in PBS (10 mM, pH 7).

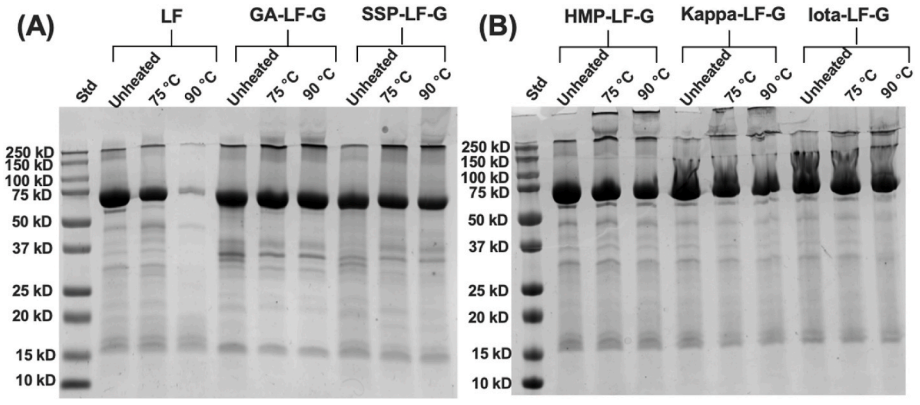

Fig. 8. Image of SDS-PAGE gels with unheated and heated (75 °C/2 min or 90 °C/2 min) LF (0.1 w/v%) and re-dispersed ternary complexes (0.2 w/v%) in PBS (10 mM, pH 7).

of peak intensity in complex samples after heating was also smaller (4.8–18.7%) than that in pure LF, except for the complex formed by SSP (Fig. 7C). Overall, the CD spectra and intrinsic fluorescence results showed that, when compared to pure LF, the LF in the ternary complex (especially GA, HMP, Kappa, or Iota system) retained more native secondary structures with less protein unfolding during the heating process.

3.6.3. LF retention in the ternary complex after thermal treatment by SDS-PAGE and HPLC analysis

SDS-PAGE and HPLC analyses was used to qualitatively and quantitively evaluate LF retention after thermal treatment. The SDS-PAGE of LF for pure unheated LF showed a distinct band at ~75 kDa (Fig. 8A) which is consistent with the molecular weight of LF as reported (Wang et al., 2019). After being heat treatment at 75 °C/2 min and 90 °C/2 min, the density of the observed LF band became significantly lighter and thinner (Fig. 8A). This result was consistent with the observed change in the CD signal and intrinsic fluorescence peak intensity of pure LF. In ternary complex samples, the LF band's density decreased in thermal-treated samples but much less than pure LF (Fig. 8A and B). The complex of GA-LF-G showed neglectable changes in the LF band after heating treatment. Other ternary complexes showed more degradation of LF compared to the GA-LF-G complex. For the Kappa-LF-G and

Table 1
LF retention ratio in LF and LF ternary complexes in PBS buffer (10 mM, pH 7) after thermal treatment (water bath, 75 °C/2 min and 90 °C/2 min) as quantified by HPLC.

Samples	LF retention % after 75 °C/2 min treatment	Samples	LF retention % after 90 °C/2 min treatment
0.2 w/v% LF	53.71 ± 1.80%^{d}	0.2 w/v% LF	4.74 ± 0.64%^{cd}
0.1 w/v% LF	52.83 ± 5.54%^{d}	0.1 w/v% LF	7.76 ± 0.96%^{c}
0.05 w/v% LF	58.56 ± 2.20%^{d}	0.05 w/v% LF	0.78 ± 0.68%^{d}
0.2w/v% GA-LF-G	100.24 ± 0.30%^{a}	0.2w/v% GA-LF-G	99.07 ± 1.15%^{a}
0.2w/v% SSP-LF-G	91.47 ± 0.82%^{b}	0.2w/v% SSP-LF-G	71.20 ± 4.79%^{b}
0.2w/v% HMP-LF-G	80.91 ± 0.46%^{c}	0.2w/v% HMP-LF-G	73.17 ± 1.47%^{b}

Different letter superscripts indicate a statistically significant difference between the mean values within each column ($P < 0.05$), compared using Tukey-Kramer HSD.

Table 2
LF retention ratio in LF and LF ternary complexes in PBS buffer (10 mM, pH 7) after thermal treatment at 145 °C for a specified amount of time as quantified by HPLC.

Samples	Time (s)	LF retention % after heating
0.1 w/v % LF	2	100.49 ± 2.85% ^{ab}
0.1 w/v % LF	10	97.08 ± 2.39% ^{bcd}
0.1 w/v % LF	30	16.48 ± 0.28% ^{g}
0.1 w/v % LF	60	7.76 ± 0.11% ^{h}
0.2 w/v % GA-LF-G	2	100.90 ± 0.38%^{a}
0.2 w/v % GA-LF-G	10	99.94 ± 0.70% ^{ab}
0.2 w/v % GA-LF-G	30	98.34 ± 1.16% ^{abc}
0.2 w/v % GA-LF-G	60	84.06 ± 1.32% ^{e}
0.2 w/v % HMP-LF-G	2	100.72 ± 0.24% ^{ab}
0.2 w/v % HMP-LF-G	10	95.55 ± 0.44% ^{cd}
0.2 w/v % HMP-LF-G	30	93.83 ± 0.54% ^{d}
0.2 w/v % HMP-LF-G	60	80.05 ± 0.82% ^{f}

Different letter superscripts indicate a statistically significant difference between the mean values ($P < 0.05$), compared using Tukey-Kramer HSD.

Iota-LF-G complexes, there was an obvious tailing of the band in the SDS-PAGE in both unheated and heated samples. This may result from the strong binding interactions between LF and the negative sulfate groups of carrageenan, which affected the separation of LF molecules in the SDS-PAGE.

HPLC analysis was used to quantify the amount or ratio of LF retained in the complexes after thermal treatment (Table 1). We focused on the ternary complex of GA-LF-G, SSP-LF-G, and HMP-LF-G before and after thermal treatment because the strong binding interactions between LF and the Kappa and Iota carrageenans interfered with our current method. The LF retention ratio in pure LF was analyzed first at different concentrations to check if concentration has a significant effect on the LF retention during heating. LF in the concentrations of 0.05–0.2 w/v % in PBS buffer (pH 7) had only half of the LF retained after being heated at 75 °C/2 min, while almost all the LF was denatured after being heated at 90 °C/2 min, with less than 10% of the LF retained at all studied concentrations (Table 1). Conversely, the LF in the ternary complexes studied was only slightly degraded with 80–100% retention of LF after being heated at 75 °C/2 min and 70–99% retention at 90 °C/2 min. Specifically in the GA-LF-G ternary complex, LF was barely degraded in both heating conditions, showing the highest LF thermal stability among all ternary complex samples. A comparison between the LF ternary complexes and the common binary complex (LF with GA, SSP and HMP) were also conducted, and the results showed that binary complex had an LF retention of 70–80% and 50–60% after being heated at 75 °C/2 min and 90 °C/2 min, respectively (data not shown), both of which is lower than our ternary complexes. Overall, the HPLC analysis proved that native LF was well-retained in the ternary complexes and that the ternary complexes also exhibited a higher LF retention than the commonly used binary systems. The enhanced LF thermal stability in ternary complex can be attributed to the additional complexation interaction from the additional biopolymers. In addition to the interactions between LF and the PS, the interaction between gelatin and the PS enhances the interpolymeric interactions within the complex strengthening the protection around LF and restricting protein structural changes during thermal treatment.

Considering the common usage of ultra-high temperature (UHT) treatment in industrial food processing, the thermal stability of LF under a higher heating temperature at ~ 145 °C for 0–60 s was investigated (Table 2). LF solutions started to show observable denaturation or loss of native LF after being heated in oil bath for 30 s with 16.5% retention, and by 60 s with only 7.8% retention as found by HPLC analysis. The GA-LF-G ternary complex showed little change after heating for 30 s at 145 °C, while the HMP-LF-G ternary complexes were less resilient only remaining intact for 10 s. Both complexes showed a significant decrease of LF retention (84.1% for GA-LF-G and 80.0% for HMP-LF-G) after 60 s of UHT treatment. The turbidity and particle size changes of the LF and ternary complex solutions were also analyzed, showing consistent results with the LF retention analysis (Fig. S3). Specifically, LF solution showed a significant increase of turbidity (Fig. S3-A and B) and mean particle size (Figs. S3–C) after 30 s treatment, while ternary complexes showed neglectable changes of turbidity and particle size after 60 s at 145 °C. The ternary complexes maintained the stability of LF even under high temperature conditions.

3.7. Amicrobial properties of LF in the ternary complex before and after thermal treatment

LF is known to exhibit anti-bacterial capacity against both gram-positive and gram-negative bacteria, retaining these properties while increasing heat stability is one of the goals of this work (Ochoa & Cleary, 2009; Ostan et al., 2017). The mechanism of the antibacterial activity of LF is currently not well understood. One mechanism proposes that the high affinity of LF causes iron deficiency in the bacteria and thus slows the bacterial growth rate (Law & Reiter, 1977). A second proposed mechanism suggests that the highly charged groups of LF may interact with the lipopolysaccharides or lipoproteins in the bacteria cell membrane thus inactivating them (González-Chávez et al., 2009). In the current work, the influence of complexation on the antibacterial activity of LF was evaluated in the ternary complexes before and after heat treatment.

S. aureus was chosen as the target Gram-positive bacteria considering it is one of the most common pathogens in dairy foods. First, the minimal inhibitory concentration (MIC) of LF on *S. aureus* was identified (Fig. 9A), which is defined as the minimal concentration of LF that was able to inhibit half of the bacterial growth compared to the control group (Matijašić et al., 2020). The MIC of LF on *S. aureus* was 0.1 w/v % after a 24 h incubation. Therefore, to be consistent with the thermal treatment in previous sections, 0.1 w/v % of LF was chosen as the study concentration and 0.2 w/v % was chosen as the complex concentration since the mass ratio of LF in the complexes was ~50%. Using an increase in the UV absorbance at 625 nm as an indicator of bacterial growth, native LF at 0.1 w/v % in PBS buffer was observed to inhibit bacterial growth by 50%, with half the value of OD625 as compared to control (Fig. 9B).

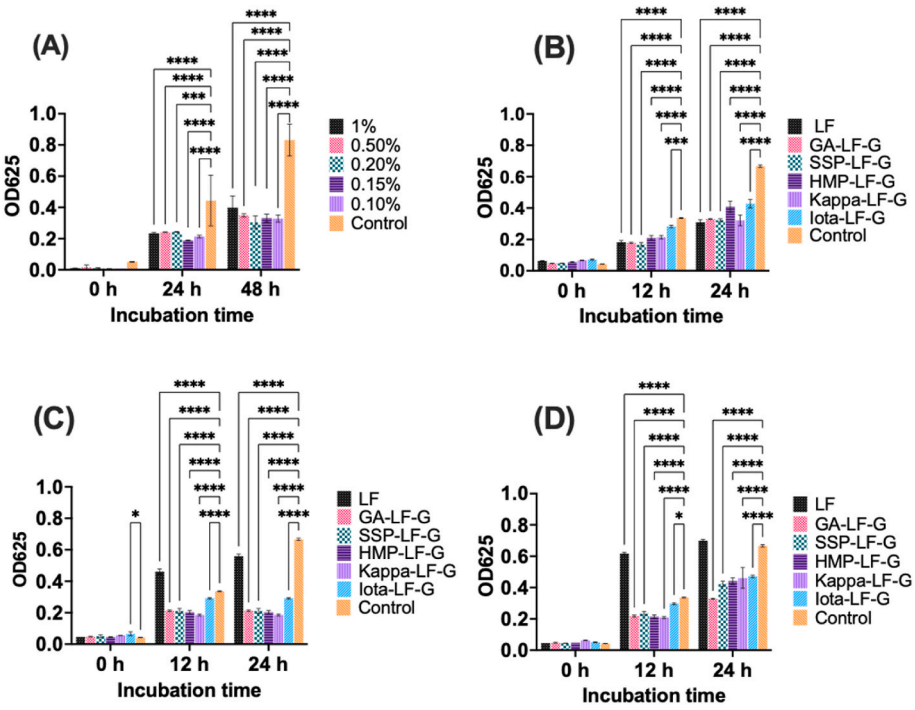

Fig. 9. The growth of *Staphylococcus aureus* as indicated by OD625. (A) incubation at 37 °C with LF for 0 h, 24 h, or 48 h of incubation at 37 °C with LF at a series of concentrations (w/v %). Incubation at 37 °C of LF (0.1 w/v %) and re-dispersed ternary complexes (0.2 w/v %) in PBS (10 mM, pH 7) (B) before thermal treatment (C) after thermal treatment at 75 °C/2 min (C) and after thermal treatment at 90 °C/2 min (D). The pairwise comparison between each sample and control was performed and the significance difference level was shown as * ($p \leq 0.05$), ** ($p \leq 0.01$), *** ($p \leq 0.001$), or ****($p \leq 0.0001$).

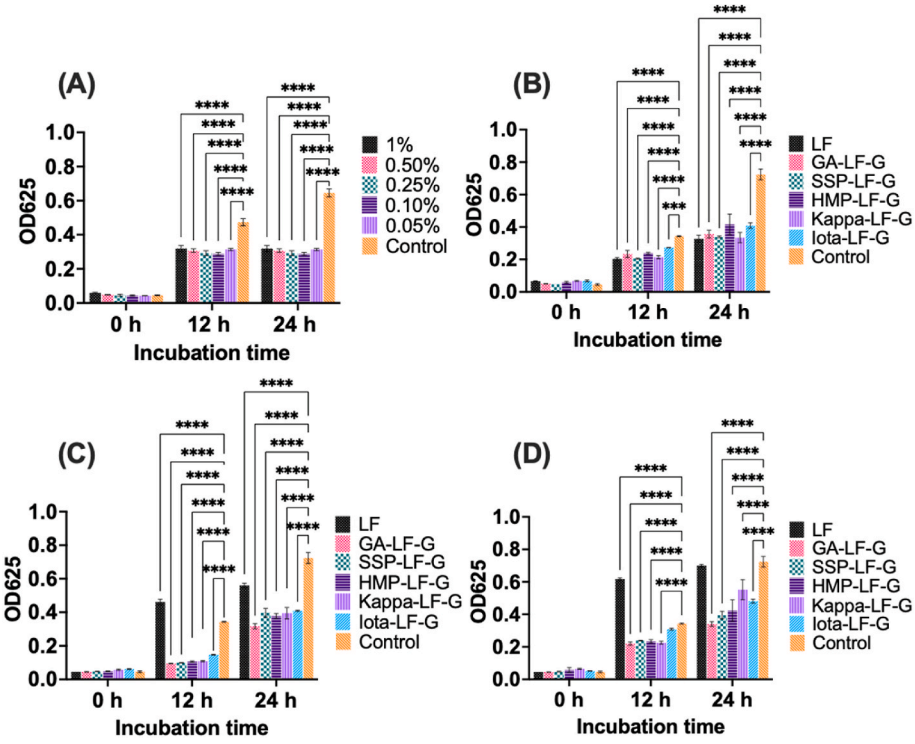

Fig. 10. The growth of *Escherichia coli* as indicated by OD625. (A) Incubation at 37 °C with LF at a series of concentrations (w/v%) for 0 h, 12 h, or 24 h. Incubation at 37 °C with LF (0.1 w/v%) and with re-dispersed ternary complex (0.2 w/v%) in PBS (10 mM, pH 7) (B) before thermal treatment (C) after thermal treatment at 75 °C/2 min, and (D) after thermal treatment at 90 °C/2 min (D). The pairwise comparison between each sample and control was performed and the significance difference level was shown as * ($p \leq 0.05$), ** ($p \leq 0.01$), *** ($p \leq 0.001$), or ****($p \leq 0.0001$).

Pure polysaccharides and gelatin did not exhibit any antibacterial effect and even promoted bacterial growth (data not shown) as they could be consumed by bacteria as energy sources. Our initial ternary complexes showed a similar OD625 as that of native LF confirming that the LF functionality was well retained after LF formed ternary complexes before heat treatments.

Native LF inhibited the bacteria growth while heat treated LF lost inhibition capacity after thermal treatment at 75 °C/2 min (Figs. 9C) and 90 °C/2 min (Fig. 9D). The impact of thermal treatments on the loss of antibacterial activity of LF has been reported previously and the antibacterial activity of LF was better preserved in pasteurized milk than in UHT milk due to the higher heating temperature in the latter conditions (Conesa et al., 2008, 2010; Niu et al., 2019). All thermally treated ternary complexes produced here demonstrated an increased antibacterial effect. The improved antibacterial effect after heat treatment at 75 °C is attributed to the degradation of the ternary complex structures and the partial exposure or release of LF during the heating process, which promoted interactions between LF and the bacteria (Fig. 9C).

Nevertheless, at 90 °C the partial denaturation of LF caused a significant decrease in the antibacterial activity of the ternary complexes (Fig. 9D).

E. coli is a common spoilage Gram-negative bacterium in food products; therefore, we also tested the antibacterial activity of LF and our ternary complexes against *E. coli*. Within 24 h incubation time, OD625 of *E. coli* in control samples was slightly higher than that of *S. aureus*, representing the generally faster bacterial growth rate of *E. coli* than *S. aureus* (Figs. 9A and 10A). Although the MIC of LF on *E. coli* was similar to the MIC of LF on *S. aureus,* around 0.1 w/v %, the antibacterial effect of LF on *E. coli* was weaker than that on *S. aureus* since the *E. coli* samples all showed a higher OD625 value after a 24 h incubation. Higher environmental resistance of Gram-negative bacteria than Gram-positive bacteria is attributed to the protective, impenetrable cell wall of Gram-negative bacteria which is surrounded by an outer membrane that Gram-positive bacteria lack (Breijyeh et al., 2020). For unheated samples, both LF and LF ternary complex demonstrated antibacterial effect on *E. coli* within a 24 h incubation (Fig. 10B). Similar to the results on *S. aureus*, heated LF samples lose antibacterial effect on *E. coli* after heat treatment due to the heat denaturation of LF (Fig. 10 C and D) while the ternary complexes retained antibacterial effect showing significantly lower OD625 values than the control. Overall, this part of the study confirmed that pure LF reduced and even lost its antibacterial capacity on both *S. aureus* and *E. coli* after heating treatment, while its antibacterial capacity was well-preserved in the ternary complex before and after heating.

4. Conclusions

A novel ternary complex was formed between LF, gelatin, and polysaccharides varying in different chain flexibilities and charge densities. The optimal condition (ratios, pH, and concentrations) to form a ternary complex for each ternary system was identified according to the ternary plots. The branched and less charged GA and SSP formed coacervate complexes with LF and gelatin at a total concentration of 1 w/v %. Linear, highly charged HMP, Kappa and Iota formed interpolymeric complexes with LF and gelatin at a total concentration of 0.2 w/v %. The formed ternary complex samples helped retain the native LF structures according to CD spectroscopy and HPLC analysis even after thermal treatments up to 90 °C under neutral pH conditions, with the GA-LF-G complex demonstrating the least thermal denaturation and structural changes of LF. Ternary complex retained a high LF retention (>90%) under UHT treatment (145 °C) for 30s. After pasteurization processing (75 °C/2 min and 90 °C/2 min), the ternary complexes formed by GA, SSP, and HMP were shown to maintain a significant antibacterial capacity of LF on both Gram-positive and Gram-negative bacteria. GA, LF, and gelatin were able to form a special multiphase coacervate with a unique coacervate-in-coacervate structure where the GA-LF coacervate tended to be inside the core of the GA-gelatin coacervate. To the best of our knowledge, it is the first time that this kind of multiphase coacervate was observed in food grade biopolymers (GA-LF-G complex), specifically protein-polysaccharides systems. The formation mechanisms and rules for the multiphase coacervate structures are still under investigation. Because multiphase coacervate structures may protect bioactive cargo in the inner coacervate layers, they may have more advanced potential to deliver bioactive components under environmental stressors: heat and enzymes. Further, the platform for designing ternary polyelectrolyte complexes using ternary plots can also be used to encapsulate other charged proteins and peptides for improved stability and functionality.

Author contributions

T. Lin: Conceptualization, data curation, formal analysis, investigation, methodology, writing-original draft, writing-review & editing; Y. Zhou: Formal analysis, methodology, investigation, writing-review & editing; Y. Dadmohammadi: Conceptualization, project administration, writing-review & editing; M. Yaghoobi: Data curation; G. Meletharayil: Resources, writing-review & editing; R. Kapoor: Resources, writing-review & editing; A. Abbaspourrad: Funding acquisition, resources, supervision, writing-review & editing.

Declaration of competing interest

The authors have no conflicts of interest to declare.

Data availability

Data will be made available on request.

Acknowledgments

This work is funded by Dairy Management Inc. (Rosemont, IL). Thanks Rebecca Zawistowski (from Dr. Crane's lab) for assistance in the CD spectroscopy. This work made use of the Cornell Center for Materials Research Shared Facilities which are supported through the NSF MRSEC program (DMR-1719875) and Imaging data was acquired through the Cornell University Biotechnology Resource Center, with NIH S10RR025502 funding for the shared Zeiss LSM 710 Confocal.

Appendix A. Supplementary data

Supplementary data to this article can be found online at https://doi.org/10.1016/j.foodhyd.2023.109064.

References

Anema, S. G., & de Kruif, C. G. (Kees) (2014). complex Coacervates of lactotransferrin and b-lactoglobulin. *J. Colloid Interface Sci., 430*, 214–220. https://doi.org/10.1016/j.jcis.2014.05.036

Balcão, V. M., Costa, C. I., Matos, C. M., Moutinho, C. G., Amorim, M., Pintado, M. E., Gomes, A. P., Vila, M. M., & Teixeira, J. A. (2013). Nanoencapsulation of bovine lactoferrin for food and biopharmaceutical applications. *Food Hydrocolloids, 32*(2), 425–431. https://doi.org/10.1016/j.foodhyd.2013.02.004

Black, K. A., Priftis, D., Perry, S. L., Yip, J., Byun, W. Y., & Tirrell, M. (2014). Protein encapsulation via polypeptide complex coacervation. *ACS Macro Letters, 3*(10), 1088–1091. https://doi.org/10.1021/mz500529v

Blocher McTigue, W. C., & Perry, S. L. (2020). Protein encapsulation using complex coacervates: What nature has to teach us. *Small, 16*(27), Article 1907671. https://doi.org/10.1002/smll.201907671

Bokkhim, H., Bansal, n., Grøndahl, L., & Bhandari, B. (2016a). Characterization of alginate-lactoferrin beads prepared by extrusion gelation method. *Food Hydrocolloids, 53*, 270–276. https://doi.org/10.1016/j.foodhyd.2014.12.002. Scopus.

Bokkhim, H., Bansal, N., Grøndahl, L., & Bhandari, B. (2016b). In-vitro digestion of different forms of bovine lactoferrin encapsulated in alginate micro-gel particles. *Food Hydrocolloids, 52*, 231–242. https://doi.org/10.1016/j.foodhyd.2015.07.007

Bradford, M. M. (1976). A rapid and sensitive method for the quantitation of microgram quantities of protein utilizing the principle of protein-dye binding. *Analytical Biochemistry, 72*(1), 248–254. https://doi.org/10.1016/0003-2697(76)90527-3

Breijyeh, Z., Jubeh, B., & Karaman, R. (2020). Resistance of gram-negative bacteria to current antibacterial agents and approaches to resolve it. *Molecules, 25*(6), 1340. https://doi.org/10.3390/molecules25061340

Bungenberg de Jong, H. G., & Kruyt, H. R. (1929). Coacervation (partial miscibility in colloid systems). *Proceedings of the Koninklijke Nederlandse Akademie van Wetenschappen, 32*, 849–856.

Chang, L.-W., Lytle, T. K., Radhakrishna, M., Madinya, J. J., Vélez, J., Sing, C. E., & Perry, S. L. (2017). Sequence and entropy-based control of complex coacervates. *Nature Communications, 8*(1). https://doi.org/10.1038/s41467-017-01249-1. Article 1.

Conesa, C., Rota, C., Castillo, E., Pérez, M. D., Calvo, M., & Sánchez, L. (2010). Effect of heat treatment on the antibacterial activity of bovine lactoferrin against three foodborne pathogens. *International Journal of Dairy Technology, 63*(2), 209–215. https://doi.org/10.1111/j.1471-0307.2010.00567.x

Conesa, C., Rota, M. C., Pérez, M.-D., Calvo, M., & Sánchez, L. (2008). Antimicrobial activity of recombinant human lactoferrin from Aspergillus awamori, human milk lactoferrin and their hydrolysates. *European Food Research and Technology, 228*(2), 205–211. https://doi.org/10.1007/s00217-008-0924-9

David, S., Wojciechowska, A., Portmann, R., Shpigelman, A., & Lesmes, U. (2020). The impact of food-grade carrageenans and consumer age on the in vitro proteolysis of whey proteins. *Food Research International, 130*, Article 108964. https://doi.org/10.1016/j.foodres.2019.108964

Fisher, R. S., & Elbaum-Garfinkle, S. (2020). Tunable multiphase dynamics of arginine and lysine liquid condensates. *Nature Communications, 11*(1), 4628. https://doi.org/10.1038/s41467-020-18224-y

Freddolino, P. L., Amini, S., & Tavazoie, S. (2012). Newly identified genetic variations in common Escherichia coli MG1655 stock cultures. *Journal of Bacteriology, 194*(2), 303–306. https://doi.org/10.1128/JB.06087-11

Goulding, D. A., O'Regan, J., Bovetto, L., O'Brien, N. M., & O'Mahony, J. A. (2021). Influence of thermal processing on the physicochemical properties of bovine lactoferrin. *International Dairy Journal, 105001*. https://doi.org/10.1016/j.idairyj.2021.105001

IDFA. (2022). *Pasteurization. IDFA-international dairy foods association*. July 22 https://www.idfa.org/news/pasteurization.

Jones, O. G., Lesmes, U., Dubin, P., & McClements, D. J. (2010). Effect of polysaccharide charge on formation and properties of biopolymer nanoparticles created by heat treatment of β-lactoglobulin–pectin complexes. *Food Hydrocolloids, 24*(4), 374–383. https://doi.org/10.1016/j.foodhyd.2009.11.003

de Jong, S., & van de Velde, F. (2007). Charge density of polysaccharide controls microstructure and large deformation properties of mixed gels. *Food Hydrocolloids, 21*(7), 1172–1187. https://doi.org/10.1016/j.foodhyd.2006.09.004

Kendre, P. N., & Satav, T. S. (2019). Current trends and concepts in the design and development of nanogel carrier systems. *Polymer Bulletin, 76*(3), 1595–1617. https://doi.org/10.1007/s00289-018-2430-y

Lin, T., Dadmohammadi, Y., Davachi, S. M., Torabi, H., Li, P., Pomon, B., Meletharayil, G., Kapoor, R., & Abbaspourrad, A. (2022). Improvement of lactoferrin thermal stability by complex coacervation using soy soluble polysaccharides. *Food Hydrocolloids*. , Article 107736. https://doi.org/10.1016/j.foodhyd.2022.107736

Lin, T., Meletharayil, G., Kapoor, R., & Abbaspourrad, A. (2021). Bioactives in bovine milk: Chemistry, technology, and applications. *Nutrition Reviews, 79*(Supplement_2), 48–69. https://doi.org/10.1093/nutrit/nuab099

Lu, T., & Spruijt, E. (2020). Multiphase complex coacervate droplets. *Journal of the American Chemical Society, 142*(6), 2905–2914. https://doi.org/10.1021/jacs.9b11468

Ma, G. (2014). Microencapsulation of protein drugs for drug delivery: Strategy, preparation, and applications. *Journal of Controlled Release, 193*, 324–340. https://doi.org/10.1016/j.jconrel.2014.09.003

Matijašić, B. B., Oberčkal, J., Mohar Lorbeg, P., Paveljšek, D., Skale, N., Kolenc, B., Gruden, Š., Poklar Ulrih, N., Kete, M., & Zupančič Justin, M. (2020). Characterisation of lactoferrin isolated from acid whey using pilot-scale monolithic ion-exchange chromatography. *Processes, 8*(7). https://doi.org/10.3390/pr8070804. Article 7.

McClements, D. J. (2018). Encapsulation, protection, and delivery of bioactive proteins and peptides using nanoparticle and microparticle systems: A review. *Advances in Colloid and Interface Science, 253*, 1–22. https://doi.org/10.1016/j.cis.2018.02.002

McTigue, W. C. B., & L. Perry, S. (2019). Design rules for encapsulating proteins into complex coacervates. *Soft Matter, 15*(15), 3089–3103. https://doi.org/10.1039/C9SM00372J

Mirabelli, C., Wotring, J. W., Zhang, C. J., McCarty, S. M., Fursmidt, R., Pretto, C. D., Qiao, Y., Zhang, Y., Frum, T., Kadambi, N. S., Amin, A. T., O'Meara, T. R., Spence, J. R., Huang, J., Alysandratos, K. D., Kotton, D. N., Handelman, S. K., Wobus, C. E., Weatherwax, K. J., … Sexton, J. Z. (2021). Morphological cell profiling of SARS-CoV-2 infection identifies drug repurposing candidates for COVID-19. *Proceedings of the National Academy of Sciences, 118*(36). https://doi.org/10.1073/pnas.2105815118

Mountain, G. A., & Keating, C. D. (2020). Formation of multiphase complex coacervates and partitioning of biomolecules within them. *Biomacromolecules, 21*(2), 630–640. https://doi.org/10.1021/acs.biomac.9b01354

Niu, Z., Loveday, S. M., Barbe, V., Thielen, I., He, Y., & Singh, H. (2019). Protection of native lactoferrin under gastric conditions through complexation with pectin and chitosan. *Food Hydrocolloids, 93*, 120–130. https://doi.org/10.1016/j.foodhyd.2019.02.020

Osel, N., Planinšek Parfant, T., Kristl, A., & Roškar, R. (2021). Stability-indicating analytical approach for stability evaluation of lactoferrin. *Pharmaceutics, 13*(7), 1065. https://doi.org/10.3390/pharmaceutics13071065

Priftis, D., Xia, X., Margossian, K. O., Perry, S. L., Leon, L., Qin, J., de Pablo, J. J., & Tirrell, M. (2014). Ternary, tunable polyelectrolyte complex fluids driven by complex coacervation. *Macromolecules, 47*(9), 3076–3085. https://doi.org/10.1021/ma500245j

Rioux, L.-E., Turgeon, S. L., & Beaulieu, M. (2007). Characterization of polysaccharides extracted from brown seaweeds. *Carbohydrate Polymers, 69*(3), 530–537. https://doi.org/10.1016/j.carbpol.2007.01.009

Royer, C. A. (2006). Probing protein folding and conformational transitions with fluorescence. *Chemical Reviews, 106*(5), 1769–1784. https://doi.org/10.1021/cr0404390

Schmitt, C., Sanchez, C., Lamprecht, A., Renard, D., Lehr, C.-M., de Kruif, C. G., & Hardy, J. (2001). Study of β-lactoglobulin/acacia gum complex coacervation by diffusing-wave spectroscopy and confocal scanning laser microscopy. *Colloids and Surfaces B: Biointerfaces, 20*(3), 267–280. https://doi.org/10.1016/S0927-7765(00)00200-9

Scott, A. M., Wolchok, J. D., & Old, L. J. (2012). Antibody therapy of cancer. *Nature Reviews Cancer, 12*(4). https://doi.org/10.1038/nrc3236. Article 4.

da, S., Gulão, E., de Souza, C. J. F., da Silva, F. A. S., Coimbra, J. S. R., & Garcia-Rojas, E. E. (2014). Complex coacervates obtained from lactoferrin and gum Arabic: Formation and characterization. *Food Research International, 65*, 367–374. https://doi.org/10.1016/j.foodres.2014.08.024

Sreedhara, A., Flengsrud, R., Prakash, V., Krowarsch, D., Langsrud, T., Kaul, P., Devold, T. G., & Vegarud, G. E. (2010). A comparison of effects of pH on the thermal stability and conformation of caprine and bovine lactoferrin. *International Dairy Journal, 20*(7), 487–494. https://doi.org/10.1016/j.idairyj.2010.02.003

Turgeon, S. L., & Laneuville, S. I. (2009). Chapter 11 - protein + polysaccharide coacervates and complexes: From scientific background to their application as functional ingredients in food products. In S. Kasapis, I. T. Norton, & J. B. Ubbink (Eds.), *Modern biopolymer science* (pp. 327–363). Academic Press. https://doi.org/10.1016/B978-0-12-374195-0.00011-2.

Van Calsteren, M.-R., Pau-Roblot, C., Bégin, A., & Roy, D. (2002). Structure determination of the exopolysaccharide produced by Lactobacillus rhamnosus strains RW-9595M and R. *Biochemical Journal, 363*(1), 7–17. https://doi.org/10.1042/bj363007

Vergara, D., & Shene, C. (2019). Encapsulation of lactoferrin into rapeseed phospholipids based liposomes: Optimization and physicochemical characterization. *Journal of Food Engineering, 262*, 29–38. https://doi.org/10.1016/j.jfoodeng.2019.05.012

Vogel, H. J. (2012). Lactoferrin, a bird's eye view. *Biochemistry and Cell Biology, 90*(3), 233–244. https://doi.org/10.1139/o2012-016

Wang, B., Timilsena, Y. P., Blanch, E., & Adhikari, B. (2017). Mild thermal treatment and in-vitro digestion of three forms of bovine lactoferrin: Effects on functional properties. *International Dairy Journal, 64*, 22–30. https://doi.org/10.1016/j.idairyj.2016.09.001

Wang, B., Timilsena, Y. P., Blanch, E., & Adhikari, B. (2019). Lactoferrin: Structure, function, denaturation and digestion. *Critical Reviews in Food Science and Nutrition, 59*(4), 580–596. https://doi.org/10.1080/10408398.2017.1381583

Wotring, J. W., Fursmidt, R., Ward, L., & Sexton, J. Z. (2022). Evaluating the in vitro efficacy of bovine lactoferrin products against SARS-CoV-2 variants of concern. *Journal of Dairy Science*. https://doi.org/10.3168/jds.2021-21247. S0022030222001151.

Zheng, J., Gao, Q., Tang, C., Ge, G., Zhao, M., & Sun, W. (2020). Heteroprotein complex formation of soy protein isolate and lactoferrin: Thermodynamic formation mechanism and morphologic structure. *Food Hydrocolloids, 100*, Article 105415. https://doi.org/10.1016/j.foodhyd.2019.105415